*Oxidation of Metals, Vol. 36, Nos. 3/4, 1991*

# Analysis of Oxygen-18 Tracer Profiles in Two-Stage Oxidation Experiments (I): Predominant Oxygen Diffusion in the Growing Scale

**W. Wegener* and G. Borchardt***

*Received November 26, 1990; revised April 22, 1991*

*Typical two-stage oxidation experiments in high-temperature oxidation studies on metals are analyzed. Two cases of predominant oxygen diffusion in the scale are studied: pure volume diffusion and simultaneous transport via grain boundaries and via the bulk. An analytical expression for the growth of the oxide layer is given for the assumption that the chemical potential of the oxygen varies linearly over the oxide layer. The numerical treatment of the differential equation is improved so that the calculation is possibly faster and/or more accurate compared to a method given in the literature. The experimental profiles are described by four parameters, the grain boundary width, the grain radius, and the volume and grain-boundary diffusivities. Two equations correlating these parameters can be extracted from the profiles. Two benchmark tests are described for testing the program. An analytical solution is presented which approximately describes the distribution of O-18 in the oxide layer for pure volume diffusion. Experimental SIMS profiles on Fe–Cr–Al alloys are explored on the basis of our calculation.*

**KEY WORDS:** two-stage oxidation; O-18; growth mechanism; diffusion model; grain-boundary diffusion.

## INTRODUCTION

In studying oxidation mechanisms, oxygen tracer isotopes are commonly used. S. N. Basu and J. W. Halloran[1] developed a model in which the oxygen

*Arbeitsgruppe Elektronische Materialien, FB Metallurgie und Werkstoffwissenschaften, Technische Universitaet Clausthal, D-3392 Clausthal-Zellerfeld, Germany.



0030-770X/91/1000-0339$06.50/0 

was incorporated into the oxide layer via grain-boundary transport and via the exchange between the grain boundaries and spherical grains. Since the diffusion via grain boundaries is much faster than the diffusion into the volume, one would expect to have an increase in the O-18 profile near the metal/oxide interface by the formation of new oxide there. This has been seen in oxidation experiments of Fe–Cr–Al alloys (which initiated this study) and is believed to be a common feature of all oxides growing by (inward) diffusion of oxygen.

In implementing the theory of Basu *et al.* in a computer program, we realized, however, that considerable improvements could be made which we will present in this paper. Moreover, we will present two bench-mark test cases for anyone who wants to develop or just use a program based on this theory. One of these is the analytical solution describing the inward oxygen volume diffusion in the presence of a gradient of the chemical potential. We will then treat a specific example and demonstrate what can be learned about the physical parameters involved.

## MODELING THE OXYGEN TRANSPORT

Basu *et al.*[1] assume that the oxide layer consists of spherical grains of radius $r$, separated by grain boundaries of width $\vartheta$. Let $X(t)$ be the thickness of the oxide layer after time $t$. The x-axis is defined by the two points $x=0$ for the oxide layer/gas interface and $x=X(t)$ for the oxide layer/alloy interface. The alloy is oxidized in a pure O-16 atmosphere for a time $t_0$. Then a pure O-18 atmosphere is introduced. The O-18 diffuses into the oxide layer via the grain boundaries; on its way to the oxide/alloy interface, it is enriched with O-16 by exchange with the O-16 from the grains. The mixture of O-18 and O-16 arriving at $x=X(t_0)$ is used to build up new oxide and therefore the interface $x=X(\mathrm{t})$ is a moving one. In this model, it is therefore assumed that the oxide layer grows by inward oxygen diffusion. There are two driving forces for this inward diffusion. The first driving force is the difference in the chemical potential of the oxygen at the gas/oxide interface and at the oxide/alloy interface $\Delta\mu$. The second driving force is the gradient of the O-18 concentration within the grains and between a grain and a grain boundary.

To model this process one has to answer two questions, namely, which differential equation governs the situation in the grain boundary and what is the growth rate?

### The Treatment of Basu *et al.*

As a basis for further discussion we now shortly describe the solution given by Basu *et al.*[1] The underlying assumptions and their implications are discussed in the next section.

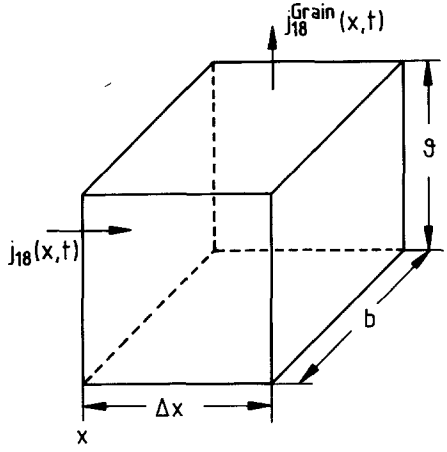


**Fig. 1.** Small volume element of the grain boundary. Graphical visualization of $\vartheta$, $\Delta x$, and $b$.

To develop a differential equation for the oxygen transport in the grain boundary, we consider a small volume element (Fig. 1). If $j_{18}(x, t)$ is the current of O-18 atoms per unit area and unit time within the grain boundary, and $j_{18}^{\text{Grain}}(x, t)$ is the current into the grain per unit area and unit time, then the increase in concentration of O-18 atoms in this volume element is given by

$$[j_{18}(x+\Delta x, t)-j_{18}(x, t)]\vartheta\, b\, \Delta t-2j_{18}^{\text{Grain}}(x, t)b\, \Delta x\Delta t=\Delta c_{18}\vartheta\, b\, \Delta x \quad (1)$$

The current density $j_{18}$ is given by

$$j_{18}=-D_{\text{gb}}\frac{\delta c_{18}}{\delta x}+\frac{D_{\text{gb}}c_{18}\,\Delta\mu}{RTX(t)} \quad (2)$$

where $R$ is the gas constant, $T$ the temperature, and $D_{\text{gb}}$ the grain boundary diffusion coefficient of oxygen. $c_{18}$ is the number of O-18 atoms per unit grain boundary volume. In this paper, $\Delta\mu$ is the absolute value of the difference of the chemical potential of oxygen at the gas/oxide interface and at the oxide/metal interface, respectively, and refers to the reaction

$$2\text{Al(s)}+\tfrac{3}{2}\text{O}_2\text{(g)}=\text{Al}_2\text{O}_3\text{(s)} \quad (3)$$

The first term on the right hand side of Eq. (2) describes the isotopic mixing of O-16 and O-18 and the second term describes the influx of oxygen in the sample due to its gradient of the chemical potential of oxygen. Since $d\mu/dx$

is written as $\Delta\mu/X(t)$, it is assumed that this gradient is constant with respect to $x$. With Eqs. (1) and (2) it follows that

$$\frac{\delta c_{18}}{\delta t} = D_{gb}\frac{\delta^2 c_{18}}{\delta x^2} - \frac{D_{gb}\Delta\mu}{RTX(t)}\frac{\delta c_{18}}{\delta x} - \frac{2}{\vartheta} j_{18}^{Grain} \tag{4}$$

Since the total oxygen concentration in the grain boundary is assumed to be independent of time and location, it follows from Eq. (4) that the flux of O-18 into the grains equals the flux of O-16 out of the grains. Equation (4) can be solved numerically, given the boundary conditions, if one knows $X(t)$ and $j_{18}^{Grain}$.

Basu *et al.* propose to calculate the latter by considering the amount of O-18 which diffuses into a spherical grain. They refer to the Oishi–Ichimura geometrical configuration,[2] in which the volume is simulated by equally-sized spherical grains which are completely surrounded by the grain boundaries. The grain boundaries are perpendicular to the oxide surface. For more details and figures, we refer the reader to Ref. 1. The amount of O-18 diffusing into a spherical grain can be calculated by procedures found in the literature.[3] If a sphere of radius $r$ has an initial tracer concentration of $c_{18}^i(t)$ and the concentration at the surface of the sphere is raised at time $t = t_0$ from $c_{18}^i$ to $c_{18}^f$, then the amount of O-18 in the sphere at a time $t \geq t_0$ is given by:

$$M(t) = \left[1 - \frac{6}{\pi^2}\sum_{n=1}^{\infty}\frac{1}{n^2}\exp\left(-\frac{D^V n^2\pi^2\tau}{r^2}\right)\right]\frac{4}{3}\pi r^3(c_{18}^f - c_{18}^i) + \frac{4}{3}\pi r^3 c_{18}^i \tag{5}$$

where $\tau = t - t_0$ and $D^V$ is the volume diffusion coefficient.

The flux into the sphere can be obtained, using Fick's law, by differentiating the numerical solution for $c_{18}(x, t)$ for this problem with respect to $x$. In this way, Basu *et al.* get (Eq. (6) in Ref. 1):

$$j_{18}^{Grain}(x, t) = \frac{2D^V}{r}(c_{18}(x, t) - c_{18}^i)\sum_{n=1}^{\infty}\exp\left(-\frac{D^V n^2\pi^2\tau}{r^2}\right) \tag{6}$$

This current can be used in Eq. (4), if one assumes that the concentration at the surface of the spherical grains $c_{18}(x, t)$ is identical to the O-18 concentration within the grain boundary at any previous time $t \geq t_0$, e.g., due to a much faster grain boundary diffusion compared to volume diffusion.

The thickness of the scale inserted in Eq. (4) used by Basu *et al.* is given by

$$X(t) = (K_p(\tau + t_0))^{1/2} \tag{7}$$

where $K_p$ describes the parabolic growth rate. In this paper $t_0$ and $\tau$ are the O-16 and the O-18 oxidation time, respectively.

The average concentration as measured by a SIMS analysis is given by

$$c_{18}^{\mathrm{SIMS}} = \frac{\frac{4}{3}\pi r^3 c_{18}^{\mathrm{Grain}} + 4\pi r^2 \frac{\vartheta}{2} c_{18}}{\frac{4}{3}\pi r^3 + 4\pi r^2 \frac{\vartheta}{2}} \tag{8}$$

where $c_{18}^{\mathrm{Grain}}(x, t)$ is given by Eq. (5) divided by the volume of the sphere, i.e.,

$$c_{18}^{\mathrm{Grain}}(x, t) = \left[1 - \frac{6}{\pi^2} \sum_{n=1}^{\infty} \frac{1}{n^2} \exp\left(-\frac{D^V n^2 \pi^2 \tau}{r^2}\right)\right](c_{18}(x, t) - c_{18}^i) - c_{18}^i \tag{9}$$

It is assumed that oxygen is incorporated in a grain only via the grain boundaries, i.e., any volume diffusion parallel to the x-axis is neglected (including any O-16/O-18 exchange reaction at the surface via the volume).

Defining values for $D^V$, $D_{\mathrm{gb}}$, $\vartheta$, $K_p$, and $r$, one is therefore able to solve the differential Eq. (4) and to calculate the SIMS profile via Eq. (8).

Our intention in this section was to illustrate this model. For more details, we refer the reader to Ref. 1 and to an extensive NASA report by Basu[4] which includes a computer program.

*Discussion of the Approximations*

In developing Eq. (2), it was assumed that the gradient of the chemical potential of oxygen is constant. Thus, the treatment is confined to cases where oxygen diffuses as uncharged species or the defect concentration leading to oxygen diffusion is independent from the location. The latter can be assumed in cases where the concentration of intrinsic defects is small compared to extrinsic defects, as is the case for alumina scales on alloys where the motion of oxygen is believed to be controlled by doping, since it is virtually impossible to measure any intrinsic defects or any dependence of the corrosion constant on the partial pressure of oxygen in the gas atmosphere.

In developing Eq. (6), we used Eq. (5) which is valid only if the surface concentration of the grains, i.e. the grain boundary concentration, is brought to its final oxygen concentration immediately. Since the O-18 concentration within the grain boundary is growing monotonically, this approximation is justified in cases where the grain-boundary diffusion is much faster than the volume diffusion so that the final concentration in the grain boundary is reached fast. This is the same approximation Fisher[5] successfully used in his investigation of the diffusion of radioactive silver into a polycrystalline silver specimen. We should therefore be able to reproduce his approximate solution exactly, which we will do as a test case for the programs. This approximation also becomes better with smaller grain-boundary width compared to the

grain size since this means that at the time one measures a sizable amount of O-18 within the volume the O-18 concentration within the grain boundary had enough time to reach its final, i.e., steady state concentration. Since we are dealing with a complex situation solved by a computer simulation, it is difficult if not impossible to make these arguments more quantitative. It is therefore necessary to check the validity of this approximation using the results of the computer simulation.

In developing Eq. (8), any volume diffusion parallel to the x-axis is neglected. This approximation is justified in cases where $(2D^V t)^{1/2} \ll X(t)$, which will be calculated in the section "Analytical Expression for $X(t)$."

## Improvements of the Treatment Given by Basu *et al.*

### *Improved Calculation of $j_{18}(x, t)$*

To solve the differential equation, Eq. (4), one defines a mesh of equidistant points on the x-axis. During the O-18 oxidation period one starts with $c_{18}(x, t) = 0$ for $x > 0$, and $t = t_0$, i.e., $\tau = 0$, in the oxide scale and $c_{18}(0, \tau)/(c_{18} + c_{16}) = N_0$, where the molar fraction $N_0$ is the same as in the gas atmosphere. The increase of $c_{18}(x, t)$ within a time interval $\Delta t$, $\Delta c_{18}(x, \Delta t)$, is calculated by multiplying Eq. (4) with $\Delta t$. Since these calculations have to be done for every new time, it is of great importance to simplify the calculation at this stage. In our first calculations, we realized that calculating $j_{18}^{\text{Grain}}$ from Eq. (6) is very time consuming, if not impossible. In the beginning of the O-18 oxidation, $\tau$ is very small, so one needs a large number of terms to calculate the sum on the right hand side of Eq. (6) with sufficient accuracy. For $\tau = 0$, however, this sum diverges. In solving the differential equation Eq. (4), one does not need $j_{18}^{\text{Grain}}$, but $j_{18}^{\text{Grain}}\,\Delta t$, which even for small times is finite. We therefore calculate the amount of O-18 flowing into the sphere between time $t$ and $t + \Delta t$, i.e.,

$$4\pi r^2\,\Delta t\, j_{18}^{\text{Grain}}(x, t) = (M(t + \Delta t) - M(t)) \tag{10}$$

With Eq. (5) we get for $j_{18}^{\text{Grain}}(x, t)\,\Delta t$

$$j_{18}^{\text{Grain}}(x, t)\,\Delta t = \frac{2r}{\pi^2}\,[c_{18}(x, t) - c_{18}^{i}(x, t)]S(t) \tag{11}$$

where $S(t)$ is given by

$$S(t) = \sum_{n=1}^{\infty} \frac{1}{n^2} \exp\left[-\frac{D^V n^2 \pi^2 \tau}{r^2}\right](1 - \exp[-D^V n^2 \pi^2 \Delta t / r^2]) \tag{12}$$

with $\tau = t - t_0$.

Comparing Eqs. (11) and (6), we realize the appearance of the factor $1/n^2$ in Eq. (12), which leads to a faster convergence of the sum and therefore reduces the calculation time considerably. Moreover, it is possible to give an analytical approximation for the sum Eq. (12) (see Appendix). As we use $c_{18}$ instead of $c_{18}^f$ in Eq. (11) we apply the same approximation as Basu *et al.* did.

*Analytical Expression for $X(t)$*

To gain an analytical expression for the thickness of the oxide layer avoiding the introduction of the additional parameter $K_p$ we notice that a segment $\Delta X$ of new layer is built up within a time interval $\Delta t$ by oxygen flowing into the surface at $x=0$. Let $A^{gb}$ be the cross-section area of the grain boundary and $A$ the cross-section of the sample. Then, with the use of Eq. (2):

$$[j_{16}(0, t)+j_{18}(0, t)]A^{gb}\,\Delta t=\frac{D_{gb}\,\Delta\mu}{RT\,X(t)}\,(c_{16}(0, t)+c_{18}(0, t)]A^{gb}\,\Delta t \quad (13)$$

Eq. (13) has to be identical to $c_O^m\,\Delta X A$, where $c_O^m=c_{16}^{SIMS}+c_{18}^{SIMS}$ is the constant oxygen concentration in the oxides scale. We then obtain a diffusion equation for $X(t)$, i.e.,

$$X(t)\,\Delta X=\frac{D_{gb}\,\Delta\mu}{RT}\,\frac{A^{gb}}{A}\,\Delta t \quad (14)$$

Now the ratio of the grain-boundary volume to the total volume consistent with the model of Basu is given by

$$\frac{A^{gb}\,\Delta x}{A\,\Delta x}=\frac{4\pi r^2\vartheta/2}{\frac{4}{3}\pi r^3+4\pi r^2\vartheta/2}=\frac{3\vartheta}{2r+3\vartheta}$$

With the help of Eq. (14) we get for $X(t)$:

$$X(t)=\left(\frac{2D_{gb}\,\Delta\mu\;t}{RT}\,\frac{3\vartheta}{2r+3\vartheta}\right)^{1/2} \quad (15)$$

One realizes an interesting consequence of this. An oxygen can enter the sample from the gas atmosphere by replacing an oxygen to the gas atmosphere or by not doing this. In the presence of a gradient of the chemical potential of oxygen, the latter is possible due to growth of the oxide layer. If we assume that no oxygen from the sample is replaced to the gas atmosphere by an exchange reaction, we can compare $c_O^m[X(t)-X(t_0)]$ with $\int_0^{X(t)} c_{18}^{SIMS}(x, t)\,dx$. From the definition, $N_0=c_{18}(0, t)/[c_{18}(0, t)+c_{16}(0, t)]$, i.e., $c_{18}(0, t)+c_{16}(0, t)=1/N_0\times c_{18}(0, t)$, one can calculate the total amount

of oxygen which was incorporated into the sample per unit area from the amount of O-18. Thus, the identity

$$X(t)-X(t_0)=\frac{1}{N_0 c_O^m}\int_0^{X(t)} c_{18}^{\mathrm{SIMS}}(x, t)\,dx \tag{16}$$

should be valid. It can easily be checked by a numerical integration of the calculated O-18 concentration profile.

In general, however, i.e., if an exchange of oxygen from the sample to the gas atmosphere takes place, the right-hand side of Eq. (16) will be larger than the left-hand side, the difference becomes larger with diminishing gradient of the chemical potential of oxygen (for $\Delta\mu=0$, each O-18 entering the sample replaces oxygen to the gas atmosphere without contribution to the growth of the oxide layer). This difference is a measure of enrichment of the gas atmosphere with O-16.

## Growth by Oxygen Volume Diffusion

We now treat the situation, where the oxide layer grows by inward (volume) diffusion of oxygen. Again we consider O-16 oxidation followed by oxidation in a gas atmosphere containing O-16 and O-18.

In looking at Eq. (2), we notice that the situation can easily be simulated by writing $D^V$ instead of $D_{\mathrm{gb}}$ in the second term on the right-hand side. For this differential equation,

$$\frac{\delta c_{18}}{\delta t}=D^V\frac{\delta^2 c_{18}}{\delta x^2}-\frac{D^V\Delta\mu}{RTX(t)}\frac{\delta c_{18}}{\delta x} \tag{17}$$

even an analytical solution can be found, namely,

$$c_{18}(x, t)=\frac{c_0}{2}\,\mathrm{erfc}\left[\frac{x-\left(\frac{2D^V\Delta\mu}{RT}\right)^{1/2}(t^{1/2}-t_0^{1/2})}{2[D^V(t-t_0)]^{1/2}}\right] \tag{18}$$

$X(t)$ is taken from Eq. (15) with $\vartheta\gg r$, i.e., formally we treat the grain boundary as the volume. We have not found this solution in the literature. One reason may be that $c_{18}(x, t)$ is not a function of $x/t^{1/2}$, so a well-known substitution for diffusion-related differential equations does not lead to Eq. (18). Furthermore, Eq. (18) corresponds to the boundary conditions only approximately. For $t=t_0$ we demand $c_{18}(0, t=t_0)=c_0$, whereas Eq. (18)

yields $c_0/2$. So we have described a different sort of experiment. The difference is not great, however. Let us ask fo the time $t_{0.9}$, when $c_{18}(0, t_{0.9}) = 0.9\ c_0$. With the use of Eq. (18), it can be shown that

$$t_{0.9} = \left[\frac{1+(0.9/a)^2}{1-(0.9/a)^2}\right]^2 t_0$$

with $a = [\Delta\mu/(2RT)]^{1/2}$. For typical values of $\Delta\mu = 10^6$ J/mol/K and $T =$ 1100 °C, we turn out with $t_{0.9} = 1.08 t_0$. For an O-16 oxidation time of $t_0 =$ 1 hr, it thus takes $c_{18}(0, t)$ just 4 min to reach 0.9 $c_0$ in the subsequent O-18 oxidation. Similarily, the surface concentration of O-18 will reach 0.95 $c_0$ and 0.99 $c_0$ within 8 and 17 minutes, respectively.

The solution Eq. (18) is of importance for pure volume diffusion, because one can extract $D^V$ from the measured profile immediately. We notice that $c_{18}/[c_{18}+c_{16}] = 0.5$ is reached for $x_{1/2} = (2D^V \Delta\mu/RT)^{1/2}(t^{1/2} - t_0^{1/2})$. If $\Delta\mu$ is known, $D^V$ follows from the respective plot by measuring $x_{1/2}$. It has to be recalled that this evaluation of the volume diffusion coefficient is only justified for a situation where the chemical potential varies linearly across the oxide scale.

Equation (18) establishes an analytical solution which is well suited as a test for a computer program solving Eq. (4), since the case of volume diffusion can easily be simulated, as we will demonstrate later.

## TEST CASES FOR THE COMPUTER PROGRAM

To find errors in a complex computer program and to check the accuracy of the results, it is of great importance to have some test cases. Even in a situation where one "only" implements a program written by someone else on one's own equipment, it is of importance to check for errors. Ideally, a test case should consist in an analytical solution and probe for a complex part of the program. Since Basu *et al.*[1] did not treat such test cases, we think it is useful to add them.

We will discuss two cases. The first is a thin layer of high-diffusivity material sandwiched between large volumes of low-diffusivity material, the second is the volume-diffusion model discussed in the section "Growth by Oxygen Volume Diffusion."

### Grain-Boundary Diffusion Test

Fisher[5] treated a situation, where two large single crystals are separated by a sheet of width $\vartheta$. The diffusion of a tracer into the sheet is governed by a diffusion coefficient $D_{gb}$, the diffusion into the volume by $D^V$. The

surface is defined by $x=0$, the $x$-axis being the normal pointing toward the metal/oxide interface. In a tracer diffusion experiment the concentration of the tracer at the surface $x=0$ is raised at time $t=t_0=0$ from 0 to the constant concentration of the infinite source. The experiment is performed for a time $t_f$ at a temperature $T$. It is assumed that the sheet concentration is raised instantaneously to its final value, any volume diffusion crossing the surface $x=0$ is neglected. The same approximation was made in the theory described previously, so we should be able to reproduce Fisher's (approximate) solution exactly. Fisher's analytical solution (Eq. (11) in Ref. 5) for a time $t<t_f$,

$$c(x,t)=c(x=0,t_f)\left(\frac{t}{t_f}\right)^{1/2}\exp\left[-\left(\frac{4D^V}{\pi t}\right)^{1/4}\frac{x}{(D_{gb}\,\vartheta)^{1/2}}\right] \tag{19}$$

describes the concentration one gets by sectioning the sample. This concentration is analog to the SIMS concentration we calculated in Eq. (8).

We simulate the situation by spherical grains of radius $r=1$ cm, which are extremely large compared to the grain boundary width of $\vartheta=5\times10^{-8}$ cm. With $D^V=10^{-16}$ cm$^2/s$, $D_{gb}=10^{-10}$ cm$^2/s$, $T=478$ °C, and $t_f=63$ hr we chose the same set of parameters as Fisher in his example, i.e., the diffusion of radioactive silver into a polycrystalline silver specimen. In this test the difference in the chemical potential $\Delta\mu=0$, so we have to choose $X(t_0)$, which we did by calculating $(2D_{gb}t)^{1/2}=7\times10^{-3}$ cm. Therefore, we

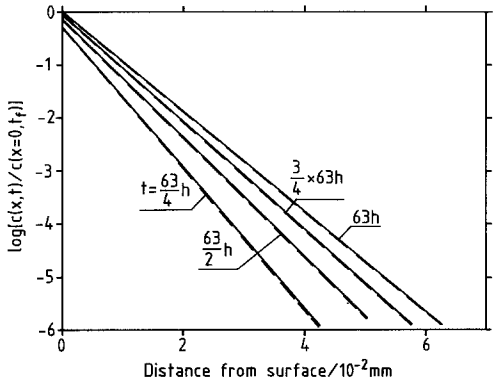


**Fig. 2.** Grain-boundary diffusion test: Comparison of Fisher's solution with that calculated by the program for $D^V=10^{-16}$ cm$^2/$s, $D_{gb}=10^{-10}$ cm$^2/$s, $\vartheta=5\times10^{-8}$ cm, $r=1$ cm, $\Delta\mu=0$ J/mol, and $T=478$ °C for four different times $(0.25, 0.5, 0.75, 1)\times63$ hr. The calculation was performed using $X(t_0)=5\times10^{-2}$ cm, sectioned in 200 meshpoints. Fisher's solution Eq. (19) is the dashed curve.

chose $X(t_0) = 5 \times 10^{-2}$ cm to approximate diffusion of the tracer into an infinite sample.

The accuracy, which can be seen from Fig. 2 is sufficient compared to experimental errors typical for diffusion experiments.

## Volume-Diffusion Test

We now refer to the situation discussed in the section "Growth by Oxygen Volume Diffusion." As we already mentioned at the end of this section, the analytical solution Eq. (18) is well suited for a test of the program. To simulate a volume-diffusion mechanism, we have to simulate a situation described by Eq. (17). This can be done by treating the grain boundary as the "volume," e.g., by keeping the volume diffusion coefficient small enough to justify neglecting the last term in Eq. (4). In this way, Eq. (4) can be transformed into Eq. (17), $D_{gb}$ now playing the role of $D^V$. Figure 3 demonstrates that the program accurately describes this situation. Moreover, the form of the profile described by Eq. (18) is visualized. It can be seen that it is indeed not difficult to extract the point $x_{1/2}$, where $c_{18}/(c_{18}+c_{16}) = 0.5$. As we discussed, one gets $D^V$ from this point immediately. One can repeat the volume-diffusion test by choosing $\Delta\mu = 0$. In this way, the second term in Eq. (17) is zero too, and Eq. (17) is transformed into

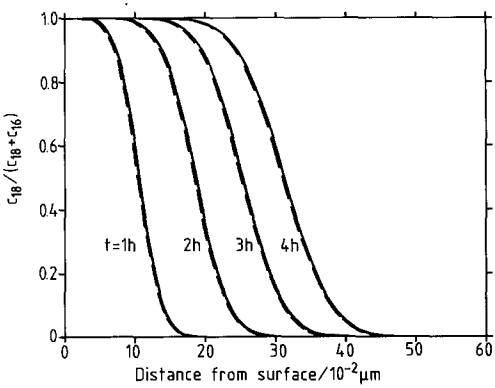


**Fig. 3.** Volume diffusion simulated in the program with the parameter set $D^V = 10^{-24}$ cm$^2$/s. $D_{gb} = 10^{-15}$ cm$^2$/s, $\vartheta = 10^{-4}$ cm, $r = 10^{-8}$ cm, $\Delta\mu = 10^6$ J/mol, $T = 1100$ °C, $t_0 = 1$ hr for four times $t - t_0 =$ (1, 2, 3, 4) hr. $X(t_0)$ was sectioned in 200 equidistant mesh points. The exact solution Eq. (18) is the dashed curve.

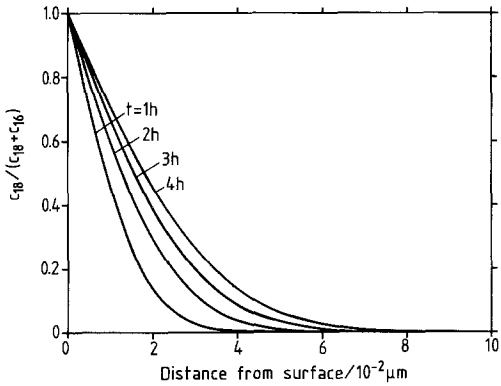


**Fig. 4.** Volume diffusion simulated using the same set of parameters as Fig. 3, but with $\Delta\mu = 0$ J/mol. $X(t_0) = 10^{-5}$ cm was subsectioned in 200 equidistant mesh points. Exact solution Eq. (20) (dashed) cannot be seen differently.

Fick's second law. With the boundary conditions we use here, the solution is straightforward and given by:

$$c_{18}(x, t) = c_0 \times \mathrm{erfc}\left[\frac{x}{2(D^V(t-t_0))^{1/2}}\right] \tag{20}$$

The result is graphically demonstrated in Fig. 4 and again shows the correctness of the program. Since we chose $\Delta\mu = 0$, we have to fix $X(t)$ in compliance with the condition $(2D^V t)^{1/2} < X(t)$ to simulate a semi-infinite sample.

## SIMULATION OF TRACER PROFILES

In this section we want to demonstrate the influence of the parameters $D^V$, $D_{gb}$, $\vartheta$, and $r$ on the profiles. To do this, we recalculated the profiles of Basu *et al.*[1,4] as an additional test and will follow their discussion.

We started with their Fig. 5 in Ref. 1 (which is identical to Fig. 14 in Ref. 4), which we compared with our results using the same set of parameters (see Fig. 5). One realizes that the difference of both profiles for $X = 0$ is negligible, whereas the tendency of the profiles is the same. However, for the times chosen in this example (18 hr O-16 oxidation time followed by 14 hr for the O-18 oxidation) one realizes the breakdown of the mass balance. We would assume that the thickness of the new-layer width can be obtained from $X(t)/X(t_0) = [(18+14)/18]^{1/2} = 1.33$ according to the parabolic time law of growth (see Eq. 15). Since $N_0 = 1$ is assumed, $1/N_0 c_0^m \times \int_0^{X(t)} c_{18}^{\mathrm{SIMS}}(x, t)\, dx = 0.33$ would be expected (see Eq. 16), if there

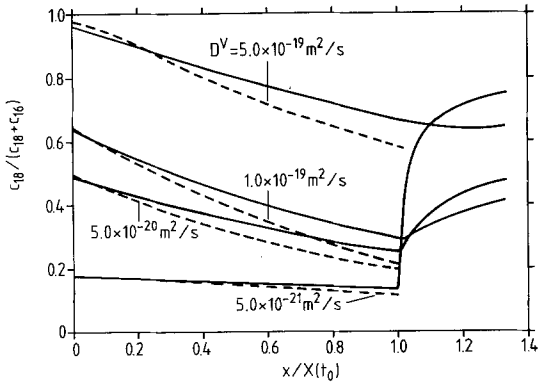


**Fig. 5.** Calculation of O-18 profiles for different volume diffusion coefficients. The parameters chosen were: $D_{gb} = 1.3\times10^{-12}\,cm^2/s$, $r = 3\times10^{-5}\,cm$, $\vartheta = 10^{-7}\,cm$, $\Delta\mu = 789{,}000\,J/mol$, $T = 1100\,°C$, $\tau = 14\,hr$, $t_0 = 18\,hr$. $X(t_0)$ was subsectioned in 100 meshpoints. Broken lines indicate results by Ref. 1. The profiles are normalized such that $X(t_0) = 1$.

is no replacement of oxygen from the sample to the gas atmosphere. However, this not the case, the difference becoming larger with increasing volume diffusivity. We recall the underlying approximation that within the grain boundary the concentration $c_{18}(x, t)$ at time $t$ is reached immediately, i.e., it is assumed to be identical to the O-18 concentration at any previous time with $\tau = t - t_0 \geq 0$. The SIMS concentration at time $t$ in Eq. (8) is calculated with the $c_{18}(x, t)$ replacing $c^f_{18}$ in Eq. (5) which obviously is higher than the concentration at any previous time. On the other hand, the differential equation Eq. (4) we are solving guarantees the balance of O-18 flowing into a volume element of the grain boundary and of the O-18 flowing out. However, $j^{Grain}_{18}(x, t)$ appearing in the differential Eq. (4) is calculated with the actual, monotonically increasing concentration $c_{18}$ in Eq. (6) and Eq. (11), respectively. Therefore the amount of O-18 which has flown into the volume as calculated from $4\pi r^2 \times \int_{t_0}^{t} j^{grain}_{18}\, dt$ is always smaller than that calculated from the SIMS concentration as calculated with Eq. (8) using the final (and highest) O-18 concentration. In this way the SIMS concentration as calculated with Eqs. (8, 9) overestimates the amount of O-18.

To make the argument more quantitive, we recalculated the profiles by using a form for $c^{SIMS}_{18}$ which is in accordance with the mass balance given by the differential Eq. (4). This can be done by calculating $c^{Grain}_{18}$ from

$$\tfrac{4}{3}\pi r^3 c^{Grain}_{18}(x, t) = 4\pi r^2 \int_{t_0}^{t} j^{Grain}_{18}(x, t)\, dt \qquad (21)$$

where $j^{Grain}_{18}$ is calculated using Eq. (6). Thus $c^{Grain}_{18}$ is calculated from the

amount which has flown into the volume and not from the final O-18 concentration in the grain boundary. This is a time average of $c_{18}^{\text{Grain}}$. The profiles calculated in this form are in good agreement with the mass balance requirement, indicating that the argument given above is indeed true. The right-hand side of Eq. (16) for $D^V = (5 \times 10^{-15}, 10^{-15}, 5 \times 10^{-16}, 5 \times 10^{-17})$ cm$^2$/s is larger than $X(t) - X(t_0)$ by (208, 69, 47, 11.7)% (see Fig. 5). If one calculates $c_{18}^{\text{SIMS}}$ by making use of Eq. (21), however, the right-hand side of Eq. (16) is larger only by (4.4, 3.5, 2.8, 1.1)%. The amount of O-18 which has flown into a grain boundary at the oxide/gas interface can be calculated from $\int_{t_0}^{t} j_{18}(x, t) A_{\text{gb}}\, dt$ using Eq. (2) and compared to the right-hand side of Eq. (16). In this example, it differs less than 0.7% from the right-hand side if one uses Eq. (21) for the calculation of $c_{18}^{\text{Grain}}$ (since we used 100 mesh points the error of the numerical integration is 1%, so any difference smaller than 1% would be accidental).

We would like to point out that $c_{18}^{\text{SIMS}}$ must not be calculated in this form, since using Eq. (21) is inconsistent with the framework of the theory. If $D^V$ is small or $r$ is large enough, the difference should not be large. One may use Eq. (21) for the calculation of $c_{18}^{\text{Grain}}$ to check for the difference in the profiles.

As a last example we recalculated Fig. 6 in Ref. 1. At a first look, it is surprising that all three profiles calculated with the parameter set given in Fig. 6 are identical, in sharp contrast to the profiles of Basu *et al.* However, we think this is reasonable. From Eq. (15), we see that $X(t)$ is proportional

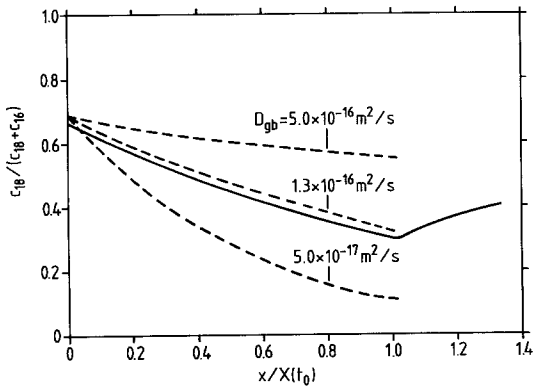


**Fig. 6.** Profiles calculated for different values of $D_{\text{gb}}$. The values chosen were: $D^V = 5 \times 10^{-16}$ cm$^2$/s, $\vartheta = 10^{-7}$ cm, $r = 2 \times 10^{-5}$ cm, $\Delta\mu = 789{,}000$ J/mol, $T = 1100$ °C, $\tau = 14$ h, $t_0 = 18$ h. $X(t_0)$ was subsectioned in 100 meshpoints. Broken lines represent the profiles of Basu *et al.*[1] The three profiles calculated by the program cannot be seen differently. The profiles are normalized so that $X(t_0) = 1$.

to $D_{gb}^{1/2}$. The amount of oxygen flowing in the sample is proportional to $D_{gb}/X(t) \propto D_{gb}^{1/2}$, as can be seen from Eq. (13), i.e., the quantity $\int_0^t c_{18}(x, t)\, dx$ is growing with exactly the same proportionally to $D_{gb}$ as $X(t)$. By normalizing the profiles so that $X(t_0) = 1$, one might therefore very well assume that the same concentration profiles for different $D_{gb}$ will be obtained.

## COMPARISON WITH EXPERIMENTS

We now want to discuss an experimental profile. We performed experiments with a Fe–Cr–Al-alloy which was oxidized in O-16 for 15 min, followed by an oxidation for 45 minutes in an atmosphere containing approximately 50 % of O-18. The experiments were performed at 1200 °C. We do not want to go into much detail here, since the experiments will be published elsewhere. We just want to demonstrate how to use the theory in a specific example, which was not possible for Basu *et al.* due to problems they describe in their paper.

In the beginning we want to mention that one has to be very careful whether the profile indicates any effect incompatible with the reasoning underlying the described theory. Since one has to calculate a profile $c_{18}/[c_{18} + c_{16}]$ from the measured $c_{18}(x, t)$ profiles, one can get the characteristic increase in the calculated profiles for larger $X(t)$ even for decreasing $c_{18}$, if the total concentration of oxygen decreases faster with increasing $X(t)$ than $c_{18}$. This can be due to cracks, grain-boundary diffusion of oxygen into the alloy, effects related with the SIMS measurements, and so forth. Since these

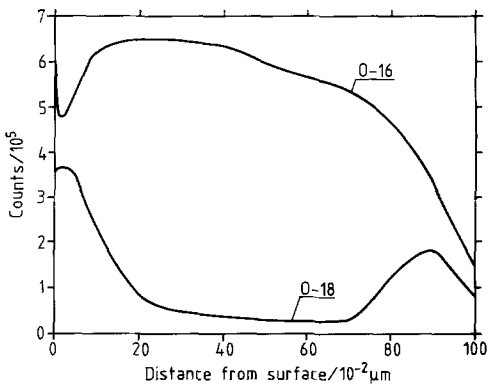


**Fig. 7.** SIMS profiles of O-16 and O-18 in a $Al_2O_3$ scale on a FeCrAl alloy at 1200 °C after oxidation in O-16 for 15 minutes, followed by an oxidation for 45 minutes in an oxygen atmosphere with 50 % O-18.

effects are not included in the theory, it is useful to apply the theory only to profiles where the concentration $c_{18}$ itself shows an increase with larger $X(t)$. This is the case in our example, as may be seen from Fig. 7.

Now we use these profiles to calculate the normalized profiles. The increase in the $c_{18}$ profiles *and* the normalized profiles indicates the end of the O-16 oxide layer $X(t_0) = 7.0 \times 10^{-5}$ cm (see Fig. 8). In the experiment we discuss here, we defined $X(t = 60 \text{ min}) = 9.7 \times 10^{-5}$ cm by the location where the oxygen concentration has half its volume value. The ratio of the total oxidation time and the O-16 oxidation time in this experiment is 4, so with Eq. (15), we would expect that $X(t) = 2X(t_0)$ which is certainly not the case here. In the framework of this theory we are therefore forced to conclude that we have an additional effect of outward diffusion of cations. To apply the theory, we took $X(t_0) - [X(t) - X(t_0)] = 4.3 \times 10^{-5}$ cm as the origin of the x-axis, i.e., as the surface of the oxide layer after the O-16 oxidation. The normalized concentration here is 0.064.

Our task now is to extract the parameters from the profiles. We assume that the surface of the sample was exposed to an O-18 concentration of 0.5. By making use of Eq. (8), we can write:

$$c_{18}^{\text{Grain}} = c_{18}^{\text{SIMS}} \left[ 1 + \frac{3\vartheta}{2r} \right] - \frac{3\vartheta}{2r} c_{18}$$

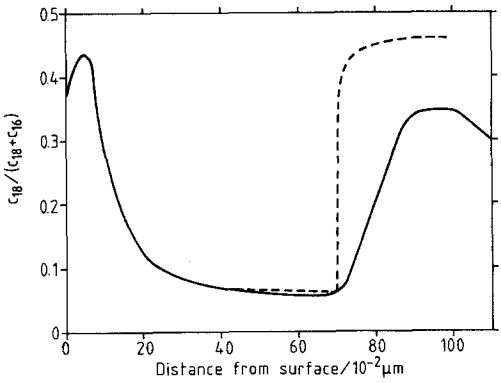


**Fig. 8.** Comparison of experimental profile with theoretical profile (dashed). The values chosen were $D^V = 2.27 \times 10^{-16}$ cm$^2$/s, $D_{gb} = 8.93 \times 10^{-13}$ cm$^2$/s, $r = 2 \times 10^{-5}$ cm, $\vartheta = 10^{-7}$ cm, $\Delta\mu = 746.470$ kJ/mol, $T = 1200$ °C, $\tau = 45$ min, $t_0 = 15$ min. $X(t_0)$ was subsectioned in 100 meshpoints. Origin of the theoretical profile at 0.43 μm.

If we assume $\vartheta/r \to 0$, we get from Eq. (5) for

$$c_{18}^{\text{Grain}} = M(t)/[4/3\pi r^3] \approx c_{18}^{\text{SIMS}}$$

$$0.064 = 0.5\left[1 - \frac{6}{\pi^2}\sum\frac{1}{n^2}\exp(-D^V\tau n^2\pi^2/r^2)\right]$$

By making a table of the term in brackets as a function of $D^V\tau/r^2$, we get

$$D^V/r^2 = 5.683 \times 10^{-7}\, s^{-1}$$

By making use of Eq. (15), we get

$$X(t_0) = \left(\frac{2D_{\text{gb}}\,\Delta\mu\; t_0}{RT}\,\frac{3\vartheta}{2r+3\vartheta}\right)^{1/2} = 2.70 \times 10^{-5}\,\text{cm}$$

The alloy we used had an aluminum content of 5 %. For the reaction

$$2\text{Al(s)} + \tfrac{3}{2}\text{O}_2\text{(g)} = \text{Al}_2\text{O}_3\text{(s)}$$

$\Delta\mu^0 = 1193.1$ kJ/Mol (see Ref. 6). Therefore $\Delta\mu$ can be obtained from

$$\Delta\mu = \tfrac{2}{3}\Delta\mu^0 + \tfrac{4}{3}RT \times \ln(x_{\text{Al}}) = 746.47\ \text{kJ/mol}$$

for $x_{\text{Al}} = 0.05$, if we assume aluminum to be solved ideally in the alloy. With $t_0 = 900$ s it follows therefore

$$\frac{3D_{\text{gb}}\vartheta}{3\vartheta + 2r} = 6.65 \times 10^{-15}\,\text{cm}^2/s$$

Now we assume $\vartheta = 1 \times 10^{-7}$ cm and $r = 2 \times 10^{-5}$ cm. It follows then $D_{\text{gb}} = 8.93 \times 10^{-13}$ cm$^2$/s and $D^V = 2.27 \times 10^{-16}$ cm$^2$/s. With this set of parameters, the profile is calculated and compared to the experimental one (see Fig. 8). Choosing a value for $r$ which is ten-fold higher results in $D^V = 2.27 \times 10^{-14}$ cm$^2$/s and $D_{\text{gb}} = 8.87 \times 10^{-12}$ cm$^2$/s. Choosing a tenfold smaller value for $D_{\text{gb}}$ results in $\vartheta = 1.07 \times 10^{-6}$ cm, $r = 2 \times 10^{-5}$ cm and $D^V = 4.49 \times 10^{-17}$ cm$^2$/s. The profiles calculated with these sets of parameters result in virtually the same profiles and are not shown in Fig. 8 separately.

It can be seen that the increase in the profile at $X(t_0)$ is too steep, whereas the overall behavior of the $c_{18}$ concentration is described. Certainly there has to be done further work to make the treatment really useful.

## CONCLUSION

We discussed a model describing the oxide-growth mechanism by diffusion of oxygen. This model contains as parameters the grain-boundary diffusivity and the volume diffusivity of oxygen, the width of the grain

boundary and the diameter of the grains. These four parameters are related by two equations and can be deduced from experiments using oxygen tracers. In the example we discussed it turned out that by variation of the two free parameters we calculated essentially the same profile. In the experiment we discussed we were forced to conclude that the model we presented is not applicable, or there is a mixed outward diffusion of metal anions and inward diffusion of oxygen. Further work has to be done, focusing on the evaluation of experimental profiles to check the applicability of the model. The size of the grains should be measured to gain additional experimental information. The variation of the grain size over the oxide layer should be included into the theory.

## APPENDIX: APPROXIMATION FOR SOME SUMMATIONS

To calculate the sum $S(t)$ in Eq. (12), we define:

$$\varepsilon = D^V \pi^2 / r^2$$

$$x_n^2 = \varepsilon \, \Delta t \, n^2$$

$$k = t/\Delta t$$

Since $\Delta n = \Delta x (\varepsilon \Delta t)^{-1/2} = 1$, we can write:

$$S(t) = (\varepsilon \, \Delta t)^{1/2} \sum_{n=1}^{\infty} \frac{1}{x_n^2} \exp(-k x_n^2)[1 - \exp(-x_n^2)] \, \Delta x \tag{22}$$

Now we define:

$$F(k, s) = (\varepsilon \, \Delta t)^{1/2} \int_0^{\infty} \frac{1}{x^2} \exp(-k x^2)[1 - \exp(-x^2 s)] \, dx \tag{23}$$

$F(k, 1)$ is larger than $S(t)$, since the integrand of Eq. (23) decreases monotonically. Taking 1 as the lower limit of the integral instead of 0, we have a lower limit for the sum. Our task is therefore to calculate Eq. (23) for $s = 1$. We differentiate $F(k, s)$ with respect to $s$ and get

$$\frac{dF}{ds} = (\varepsilon \, \Delta t)^{1/2} \int_0^{\infty} \exp(-k x^2 (k + s)) \, dx = (\varepsilon \, \Delta t)^{1/2} \frac{\pi^{1/2}}{2(k+s)^{1/2}} \tag{24}$$

Integrating this with respect to $s$ in the limits from 0 to 1 and realizing that $F(k, 0) = 0$ we turn out with an upper limit for the sum $S(t)$:

$$S^u = F(k, 1) = \pi^{1/2} (\varepsilon \, \Delta t)^{1/2} ((k+1)^{1/2} - k^{1/2}) \tag{25}$$

To get a lower limit for $S(t)$, we have to subtract

$$\alpha = (\varepsilon \, \Delta t)^{1/2} \int_0^{(\varepsilon \Delta t)^{1/2}} \frac{1}{x^2} \exp(-k x^2)(1 - \exp(-x^2) \, dx$$

which, for $(\varepsilon \, \Delta t)^{1/2} < 0.1$ can well be approximated by the error function.

We now take as an approximation for the sum the average of the upper and the lower limit. Inserting all definitions we end up with:

$$S(t) = \frac{(D^V \pi^3)^{1/2}}{r} \left[ ((t + \Delta t)^{1/2} - t^{1/2}) - \frac{\Delta t}{4 t^{1/2}} \operatorname{erf}\left( \left( \frac{D^V t}{r^2} \right)^{1/2} \pi \right) \right] \tag{26}$$

for

$$\beta = (D^V \Delta t\, \pi^2/r^2)^{1/2} \leq 0.1$$

$\Delta t$ is always be chosen to make sure $\beta \leq 0.1$. For typical values of $D^V = 10^{-15}$ cm$^2$/s and $r = 10^{-5}$ cm this means, $\Delta t$ has to be smaller that 10 s, leading to 360 iterations per hour O-18 oxidation. This proves to pose no problem at all in terms of the computing time available.

The error one makes using this approximation, is in the order of $\alpha/S^u$. For $t/\Delta t \gg 1$, one can easily show that

$$\alpha/S^u = \frac{\operatorname{erf}(D^V t\pi^2/r^2)^{1/2}}{2 - \operatorname{erf}(D^V t\pi^2/r^2)^2}$$

For $D^V t/r^2 \leq 0.0025$ this is in the order of 1 %, which we considered sufficient compared to the accuracy of the experiments. Therefore, we use the approximation Eq. (26) for times $t < 0.0025\, r^2/D^V$, otherwise the sum $S(t)$ is calculated by summing $S(t)$ up to $n = 25r/[D^V \pi^2 t]^{1/2}$.

In the same fashion, we approximate the sum in Eq. (5) for small times. With

$$\gamma = \frac{D^V \pi^2 t}{r^2}$$

we end up with:

$$\left[1 - \frac{6}{\pi^2} \sum_{n=1}^{\infty} \frac{1}{n^2} \exp\left(-\frac{D^V n^2 \pi^2 t}{r^2}\right)\right] = \pi^{1/2} \gamma^{1/2} - 0.5\gamma$$

for $\gamma \leq 0.01$, otherwise the summation is done up to $n = 25r/[D^V \pi^2 t]^{1/2}$.

## ACKNOWLEDGMENTS

The authors wish to express their thanks to J. Kruse and C. Riediger for preparing and performing the experiments and to J. Jedlinski for helpful discussions. We appreciate the assistance of S. Scherrer and S. Weber, Ecole des Mines, Nancy, France, with the SIMS measurements. We gratefully acknowledge the financial support by the Deutsche Forschungsgemeinschaft and the ERASMUS program of the European Economic Community.

## REFERENCES

1. S. N. Basu and J. W. Halloran, Tracer isotope distribution in growing oxide scales, *Oxid. Met.* **27**, 143 (1987).
2. Y. Oishi and H.Ichimura, Grain boundary enhanced interdiffusion in polycrystalline CaO-stabilised zirconia system, *J. Chem. Phys.* **71**, 5134 (1979).
3. J. Crank, *The Mathematics of Diffusion* (Clarendon Press, Oxford, 1956), p. 85.
4. S. N. Basu, *Analysis Techniques for Tracer Studies of Oxidation* (NASA Contractor Report 174796, 1984).
5. J. C. Fisher, Calculation of diffusion penetration curves for surface and grain boundary diffusion, *J. Appl. Phys.* **22**, 54 (1951).
6. D. R. Gaskell, *Introduction to Metallurgical Thermodynamics* (McGraw Hill Series in Materials Science and Engineering, Tokyo, 1973), p. 269.